Liquid Crystals
Publication details, including instructions for authors and subscription information:
http://www.informaworld.com/smpp/title~content=t713926090

Static and dynamic molecular properties of real and simulated PCH5

S. Ye. Yakovenko[a]; A. A. Minko[a]; G. Krömer[b]; A. Geiger[b]
[a] Institute of Applied Physics Problems, Minsk, Rep. Byelarus [b] Institute of Physical Chemistry, Dortmund University, Dortmund, F. R. Germany

To cite this Article Yakovenko, S. Ye. , Minko, A. A. , Krömer, G. and Geiger, A.(1994) 'Static and dynamic molecular properties of real and simulated PCH5', Liquid Crystals, 17: 1, 127 — 145
To link to this Article: DOI: 10.1080/02678299408036553
URL: http://dx.doi.org/10.1080/02678299408036553

LIQUID CRYSTALS, 1994, VOL. 17, NO. 1, 127–145

Static and dynamic molecular properties of real and simulated PCH5

by S. YE. YAKOVENKO* and A. A. MINKO
Institute of Applied Physics Problems, Kurchatova 7,
Minsk, 220064, Rep. Byelarus

G. KRÖMER and A. GEIGER
Institute of Physical Chemistry, Dortmund University,
Otto-Hahn-Strasse, D-4600 Dortmund, F. R. Germany

(*Received 10 December 1992; accepted 26 October 1993*)

We present the results of a realistic computer simulation of a liquid crystal: *trans*-4-*n*-pentyl-1-(4-cyanophenyl)cyclohexane (PCH5) and perform detailed comparisons between the molecular properties of the real and the simulated substance. With the aim of obtaining additional knowledge on its dynamic properties, the spontaneous Raman spectrum of PCH5 has been studied and the shape of the 2226 cm^{-1} band has been analysed. The data on static parameters have been taken from literature. Simulation data were obtained by a molecular dynamics method with 50 flexible molecules interacting through a site–site potential in a box with periodic boundary conditions. Analysis of static parameters $\langle D^{L}_{0m} \rangle$ and the time correlation functions $\langle D^{L}_{m0}(0) D^{L}_{m0}(t) \rangle$ (where D are Wigner functions) in the isotropic and the nematic phases on the one hand provide evidence for the advantages of the interpretation of experimental results on the basis of simulation data, and on the other hand such a comparative study helps understanding of the nature of some problems existing with regard to computer simulations of the mesophase with a realistic molecular interaction potential.

1. Introduction

When studying liquid crystalline behaviour, theoreticians and experimentalists are in substantially different situations: the former deal mainly with strongly simplified models, the latter—being faced with reality—cannot find reliable models for the treatment of experimental data. This originates from the complex balance of intermolecular forces acting between rather large and flexible mesogen molecules which leads to mesophase formation. Large molecular dimensions have restricted computer simulations of liquid crystals to geometrically simple molecular models. Therefore, being thorough and extensive (see [1, 2] and references therein) such simulations have very rarely become a useful tool for experimentalists. They give an excellent opportunity to test the theories which are based on the same molecular models, but give no possibilities for evaluating some parameters which are usually needed during the treatment of experimental data.

The necessity for a realistic treatment of the molecular structure and interactions is evident from the following examples. There was a lengthy discussion [3, 4] concerning the origin of negative P_4 order parameters as determined from Raman depolarization measurements for some substances. Many models were involved to explain this strange behaviour, but there were no reliable methods to estimate the parameters for these

* Author for correspondence.

models. Probably only for one substance has this question been answered with the help of computer simulations [5], but the others await future investigations. Very valuable information is contained in NMR spectra of liquid crystalline samples, but in order to extract either static [6] or dynamic [7] molecular parameters from them, one needs reliable data on molecular conformation in a defined phase and at a definite temperature. The same problem exists in vibrational spectroscopy. Usually severe approximations are necessary to simplify the relations between the molecular orientational correlation functions and the band-shapes of vibrational spectra [8, 9]. Some of these approximations, like the effect of molecular biaxiality, are controllable [9]; others are more speculative and the only possible way to check them is by computer simulations. The same lack of knowledge about molecular motion on the microscopic scale is felt in interpreting data for the time-resolved optical Kerr effect [10]. Also, the assignment of the bands in the far infrared spectra of such flexible molecules as mesogens [11] becomes almost totally unreliable.

And some problems face not only experimentalists, but also theoreticians. Having no reliable data on the importance of the contributions of different molecular properties to interaction models, they have to use over-simplified molecular models just in order to show what their effect can be on the static [12] and dynamic [13] properties of the molecules in the mesophase. Such examples are numerous.

Recently, some realistic computer simulations were described in the literature [5, 14–16]. But these papers are mainly devoted either to intramolecular studies or to checks on some models. The aim of this paper is to simulate a real, existing liquid crystal and to perform detailed comparisons between the molecular properties of the real and the simulated substance. We realize the difference between them, even when it is simulated with realistic intra- and inter-molecular potentials, and therefore we do not plan to involve in this comparison such macroscopic properties as elastic constants, viscosity etc, although experimental data on them are sufficiently precise. With available dimensions of the simulated ensemble, it is impossible to estimate them from simulation data without usage of models which are usually not well justified. To minimize additional possible errors, we restrict ourselves to studying the parameters of a one-particle distribution function.

We have chosen for comparative investigation the well-studied compound 4-*n*-pentyl-1-(4-cyanophenyl)cyclohexane (PCH5). While there are sufficiently extensive experimental data available in the literature for this substance, there was a need to get additional knowledge on its dynamic properties. With this aim, the spontaneous Raman spectrum of PCH5 has been studied and the shape of the 2226 cm^{-1} band has been analysed. Data on other parameters have been taken from the literature. One more feature which should be mentioned here is the convention for notations. Possibly from the point of view of convenience, for different types of experiment, the relations between statistical molecular properties and macroscopic properties are usually written in the literature in different notations. Because we are not fixed to one type of experiment, we shall adopt here an irreducible tensor notation similar to that in [17, 18] and recalculate some data and formulae available in the literature.

The plan of the paper is as follows. In § 2 we describe our method of computer simulation, and the properties of the simulated systems. The peculiarities of the computation of one-particle distribution function parameters are analysed and the results are accumulated in the table and figures. In the third part, available experimental data for static parameters are represented and methods for their extraction from experimentally measured quantities are analysed with the aim of

highlighting the possible origins of existing discrepancies. The fourth part is devoted to methods for the experimental determination of dynamic molecular properties—orientational auto-correlation functions which are compared with simulated ones. Finally, in the conclusions we summarize the actual limitations of the computer simulations as well as of the experimental methods, with the aim of elucidating the next steps to be taken in making comparative studies of the liquid crystalline state.

2. Simulations

To perform molecular dynamics simulations, i.e. to solve the classical equations of motion, the potential energy V of the system has to be known. Among manifold models developed for this (from mean-field models to *ab initio* computation of quantum chemistry) we have chosen a 'united atom' force field as sufficiently realistic, but with a reduced computation time compared to that for all-atom approaches, i.e. hydrogen atoms were included in the parameters of the carbon atoms (see figure 1). So, the total energy of the system is built up from a sum of site–site interactions, and the potential energy function for the interaction of the sites was taken in the form implemented in the GROMOS [19] code

$$V_{\text{total}} = \sum_{b} \tfrac{1}{2} k_b (b - b_0)^2 \qquad \text{bond stretching}$$

$$+ \sum_{\theta} \tfrac{1}{2} k_\theta (\theta - \theta_0)^2 \qquad \text{bond angle bending}$$

$$+ \sum_{\xi} \tfrac{1}{2} k_\xi (\xi - \xi_0)^2 \qquad \text{improper dihedral angle}$$

$$+ \sum_{\xi} \tfrac{1}{2} k_\phi [1 + \cos(n\phi - \delta)] \qquad \text{torsional angle}$$

$$+ \sum_{ij} \frac{1}{4\pi\varepsilon_0} \frac{q_i q_j}{r_{ij}} \qquad \text{Coulomb}$$

$$+ \sum_{i<j} \frac{A_{ij}}{r_{ij}^{12}} - \frac{B_{ij}}{r_{ij}^{6}} \qquad \text{Lennard-Jones}$$

where k_b, k_θ, k_ξ and k_ϕ are force constants, r_{ij} is the distance between sites i and j, q_i are partial charges, and A_{ij}, B_{ij} are the Lennard-Jones parameters. The parameters used in this potential are described in [20]. Thus we allowed for molecular flexibility and accounted for electrostatic interactions between the dipolar cyano groups.

We make use of the SHAKE method [21] to remove the high frequency bond-stretching motion, making it possible to increase the time step up to 2 fs. The molecular dynamics simulations were performed on systems containing 50 PCH5 molecules using rectangular periodic boundary conditions. The interactions are calculated with the minimum image convention, with the cut-off distance of 1 nm. We simulated the isotropic and the nematic phase at a constant temperature of 333 K and at a constant pressure of 1 atm. The isotropic phase was built by heating an ordered starting configuration to 1000 K and subsequent cooling down. After sufficient equilibration of 100 ps, the simulation time was 240 ps. The nematic system was produced by applying an external potential

$$V = k(1 - \cos^2\theta).$$

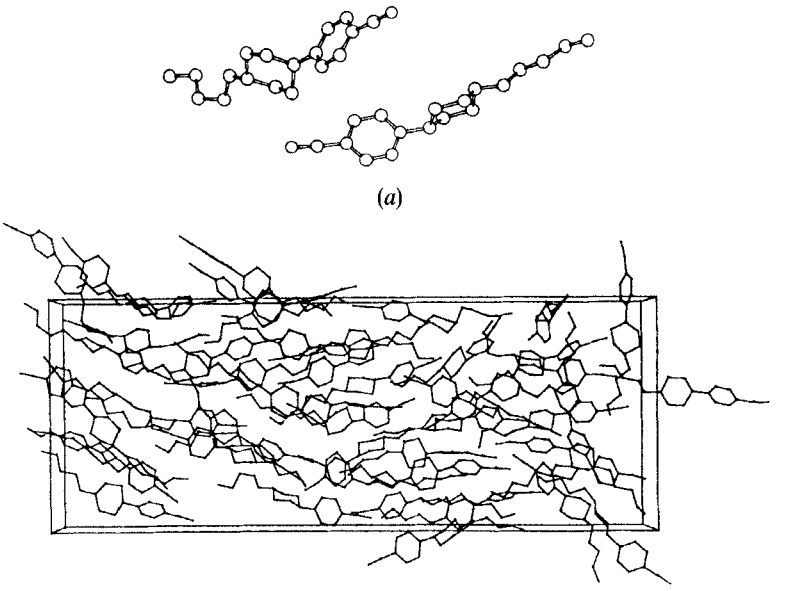

(*a*)

(*b*)

Figure 1. An example of two model molecules of PCH5 (*a*) and one of the simulated configurations (*b*). Interacting sites are depicted as balls.

where $k = 100\,\mathrm{kJ\,mol^{-1}}$, and θ stands for the angle between the C≡N bond and the z axis of the box. Afterwards followed the relaxation of the system without the extra potential for 240 ps. The behaviour of the system during the next 240 ps was studied and compared with experimental data.

For such a comparison the orientational part of the unimolecular distribution function was expanded into a set of rotational invariants [17]

$$f(\Omega) = \sum_{L=0}^{\infty} \sum_{mm'=-L}^{L} \frac{2L+1}{8\pi^2} \langle D^{*L}_{mm'} \rangle D^{L}_{mm'}(\Omega), \tag{1}$$

and a number of averages $\langle D^{*L}_{mm'} \rangle$ evaluated. Here $D^{L}_{mm'}(\Omega)$ are the Wigner functions [18] of the set of Euler angles Ω which specify the molecular orientation; angular brackets denote ensemble averaging. Since we confined ourselves to a uniaxial mesophase, $m = 0$ is considered only. In the case of a uniaxial mesophase constituted of axially symmetric molecules, $f(\Omega)$ is a function of the polar Euler angle β only and has a very simple form of expansion

$$f(\beta) = \sum_{L=\mathrm{even}} \frac{2L+1}{2} \langle P_L \rangle P_L[\cos(\beta)], \tag{2}$$

where P_L denotes Legendre polynomials and $\langle P_L \rangle = \langle D^{L}_{00} \rangle$ are the so-called order parameters. We shall refer also to $\langle D^{*L}_{mm'} \rangle$ as the order parameters. Keeping in mind that only the sum $\langle D^{L}_{mm'} \rangle + \langle D^{*L}_{mm'} \rangle$ contributes to the physical properties under study, we shall omit the complex conjugation sign, implying that only the real part of the order parameter is taken.

Time development of the P_2 order parameter for our system after 240 ps of relaxation in the nematic and isotropic phases can be seen in figure 2. We noticed that

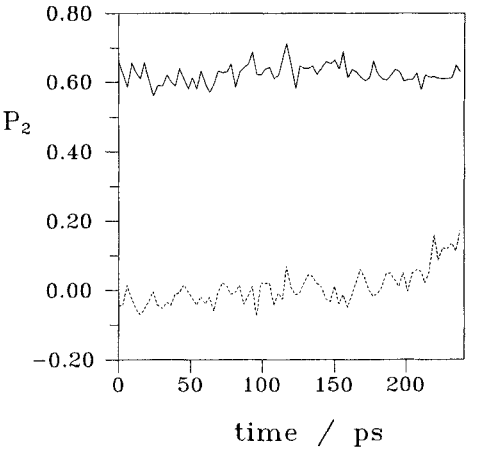

Figure 2. Time dependence of the order parameter for simulated isotropic (dashed line) and nematic (solid line) phases.

both of them possess a residual polarity: $\langle P_1 \rangle^{iso} = 0{\cdot}084$ and $\langle P_1 \rangle^{nem} = 0{\cdot}107$, respectively, but these values are within the mean-squared fluctuations for our ensemble. Concerning $P_2 = 0{\cdot}262$ in the isotropic phase, it should be noted that it is below the value at the phase transition from both theoretical and experimental points of view. The order parameters of the nematic phase (see the table) have been computed in the principle axes system of the director, which has been found to be deflected, on average, from the direction of the field which had been applied to create the ordered nematic phase. The mean-squared fluctuations of the order parameters presented in the table characterize their changes within discrete time steps. The existence of systematic deviations can be detected from the following. The simulated nematic system possesses residual biaxiality ($\langle P_2^{xx} \rangle - \langle P_2^{yy} \rangle = 0{\cdot}061$), which is sufficiently larger than the mean-square deviation of $\langle P_2 \rangle$ and can be attributed to the effect of the box boundaries.

The results, collected in the table provide evidence that, for many applications, one can neglect terms with $m' \neq 0$. Even for realistic molecular shape and interactions, their value is an order of magnitude smaller than that of the terms with $m' = 0$ of the same rank. This justifies the common practice of neglecting molecular biaxiality. Also encouraging is the relatively fast convergence of $\langle D_{00}^{L} \rangle$ (see the table): use of this property substantially simplifies theoretical description of the liquid crystalline behaviour.

Dynamic properties of molecules in the simulated systems have been computed using every tenth configuration of the simulated run—also for the nematic phase in the frame of the director. Orientational auto-correlation functions have been computed only for the C ≡ N bond because only for it are experimental data available. Results are presented in the figures and discussed in the corresponding experimental parts of the paper.

Although molecular dynamics simulation of the nematic phase has been done at the same temperature of 60°C as for the isotropic phase, i.e. above the phase transition to the isotropic liquid, the resulting system not only possess orientational order, but also this order is significantly high. Besides the inaccuracies in the potential parameters, which can only lead to a shift of the transition temperature, the most probable reason for such metastability is the strongly restricted number of molecules in the simulated

Order parameters $\langle D^{L}_{mn}\rangle \equiv Re\langle D^{L}_{mn}\rangle$ for the cyano bond of PCH5 determined in the director reference frame from molecular dynamics simulation of the nematic phase at 60°C (averaging is performed over 240 ps for 50 (the left column) and for 100 (the right column) molecules in the simulation box.

D-function	Order parameter	50 molecules	100 molecules
$\langle D^{2}_{00}\rangle$	$\frac{1}{2}\langle 3\cos^2\beta - 1\rangle$	$0{\cdot}640 \pm 0{\cdot}003$	$0{\cdot}702 \pm 0{\cdot}006$
$\langle D^{2}_{01}\rangle$	$\sqrt{\left(\frac{3}{2}\right)}\langle \cos\beta \sin\beta \cos\gamma\rangle$	$-0{\cdot}055 \pm 0{\cdot}004$	$0{\cdot}000 \pm 0{\cdot}000$
$\langle D^{2}_{02}\rangle$	$\frac{1}{2}\sqrt{\left(\frac{3}{2}\right)}\langle \sin^2\beta \cos 2\gamma\rangle$	$0{\cdot}020 \pm 0{\cdot}002$	$0{\cdot}034 \pm 0{\cdot}007$
$\langle D^{4}_{00}\rangle$	$\frac{1}{8}\langle 35\cos^4\beta - 30\cos^2\beta + 3\rangle$	$0{\cdot}327 \pm 0{\cdot}006$	$0{\cdot}403 \pm 0{\cdot}008$
$\langle D^{4}_{01}\rangle$	$\sqrt{\left(\frac{5}{2}\right)}\langle \cos\beta \sin\beta (7\cos^2\beta - 3)\cos\gamma\rangle$	$-0{\cdot}108 \pm 0{\cdot}008$	$0{\cdot}034 \pm 0{\cdot}005$
$\langle D^{4}_{02}\rangle$	$\frac{1}{4}\sqrt{\left(\frac{5}{2}\right)}\langle \sin^2\beta (7\cos^2\beta - 1)\cos 2\gamma\rangle$	$0{\cdot}020 \pm 0{\cdot}003$	$0{\cdot}015 \pm 0{\cdot}006$
$\langle D^{4}_{03}\rangle$	$\frac{\sqrt{(35)}}{2}\langle \sin^3\beta \cos\beta \cos 3\gamma\rangle$	$-0{\cdot}014 \pm 0{\cdot}004$	$-0{\cdot}018 \pm 0{\cdot}004$
$\langle D^{4}_{04}\rangle$	$\frac{1}{8}\sqrt{\frac{(35)}{2}}\langle \sin^4\beta \cos 4\gamma\rangle$	$-0{\cdot}002 \pm 0{\cdot}001$	$0{\cdot}000 \pm 0{\cdot}000$
$\langle D^{6}_{00}\rangle$	$\frac{1}{16}\langle 231\cos^6\beta - 315\cos^4\beta + 105\cos^2\beta - 5\rangle$	$0{\cdot}134 \pm 0{\cdot}007$	$0{\cdot}187 \pm 0{\cdot}007$

ensemble. This is confirmed by the strong dependence of the order parameters on the shape and dimensions of the simulated box. The right-hand column in the table represents some preliminary results for the ensemble of 100 molecules for which the order parameters should be similar or somewhat smaller than for the case of 50 molecules due to the increasing number of degrees of freedom. But some shortening of the simulation box resulted in the inverse variation, making it evident that for the anisotropic system constituted of anisotropic molecules, the choice of the shape of the box is not so trivial.

To eliminate such a strong influence of the boundaries, a substantial increase in the dimensions of the simulated ensemble is necessary, but at present that is incompatible with accessible computation time. We have chosen another way forward: we have scaled the absolute values of the order parameters, because, as will be shown, this strongly diminishes such an influence, enabling comparison with experiment, and in every case the importance of this effect is thoroughly treated.

3. Static parameters

3.1. *Raman depolarization measurements*

Since the pioneering work of Jen *et al.* [3], in which the way to use Raman depolarization measurements for the determination of order parameters has been thoroughly described, much has been done in this field (see [4, 22] and the references therein). In general, such depolarization ratios depend on a large number of orientational order parameters up to the fourth rank, but because of difficulties in their

self-consistent determination, most of the work has been done for uniaxial mesophases in the approximation of axially symmetric molecules. In our case, one can suppose that the cyano stretching vibration is coincident with the symmetry axis of the PCH5 molecule and use relatively simple formulae for the determination of the only two non-vanishing order parameters $\langle P_2 \rangle$ and $\langle P_4 \rangle$ from the Raman depolarization measurements (see, for example, [3] for the definition of r_1)

$$\left.\begin{aligned} r_1 &= \frac{\frac{1}{2}\alpha_{20}^2(\frac{1}{5}+\frac{1}{7}\langle P_2\rangle - \frac{12}{35}\langle P_4\rangle)}{\frac{1}{3}\alpha_{00}^2 + \frac{2\sqrt{2}}{3}\alpha_{00}\alpha_{20}\langle P_2\rangle + \frac{2}{3}\alpha_{20}^2(\frac{1}{5}+\frac{2}{7}\langle P_2\rangle + \frac{18}{35}\langle P_4\rangle)}, \\ r_2 &= \frac{\frac{1}{2}\alpha_{20}^2(\frac{1}{5}+\frac{1}{7}\langle P_2\rangle - \frac{12}{35}\langle P_4\rangle)}{\frac{1}{3}\alpha_{00}^2 - \frac{\sqrt{2}}{3}\alpha_{00}\alpha_{20}\langle P_2\rangle + \frac{1}{3}\alpha_{20}^2(\frac{2}{5}-\frac{2}{7}\langle P_2\rangle + \frac{27}{70}\langle P_4\rangle)}, \end{aligned}\right\} \tag{3}$$

where α_{00} and α_{20} are the spherical components (see Appendix for their relation to cartesian components) of the polarizability derivative tensor for the vibration under study. Only their ratio α_{20}/α_{00} is necessary and this can be determined from the depolarization measurements for the isotropic phase [3]. The resulting order parameters obtained in this way are presented in figure 3 (squares) and these can be compared with results by Seeliger [22] obtained by the same method, but from three depolarization ratios measurements. As argued by Seeliger, deviations of the polarizability derivatives tensor from axial symmetry has a minor effect on the results of the order parameter determination and both sets of data agree well within experimental error. The small difference should probably be attributed to different methods of Raman intensity determination (we used integral intensity in our calculations).

It should be noted that the relations (3) are valid only for the case of the so-called oriented gas. The intensity of the Raman scattering in real mesophases is modified due to their optical and molecular anisotropy [31]

$$\left.\begin{aligned} R_1 &= \frac{I_{xz}}{I_{zz}} = \frac{(n_g+n_z)^2 f_{xx}^2}{(n_g+n_x)^2 f_{zz}^2} r_1, \\ R_2 &= \frac{I_{zx}}{I_{xx}} = \frac{(n_g+n_x)^2 f_{zz}^2}{(n_g+n_z)^2 f_{xx}^2} r_2. \end{aligned}\right\} \tag{4}$$

Here n_x n_z and n_g are the ordinary and extraordinary refractive indices of the liquid crystalline sample and that of the glass cell, respectively. All of them can be determined from the refractometric measurements. The f_{ii} are the local field correction factors [3]. The data discussed in the previous paragraph have been obtained in the approximation of an isotropic local field. The main argument for this is the difficulties in the determination of the local field anisotropy, but there are also some indirect arguments for the isotropy of this field for PCH5 [4, 23].

Here we have the possibility of estimating the effect of this anisotropy by reference to some measurements for dye molecules in the PCH5 matrix [24]. There, the local field anisotropy was determined by the combination of resonance Raman scattering depolarization measurements with absorption dichroism data for the same dye molecule (DMANAB) in the mesophase of PCH5. According to the structural formulae of these substances, they have similar length to width ratios and one can presume similarity of the anisotropy of the local field acting on both types of molecules in similar surroundings. The results of the re-treatment of our Raman measurements for PCH5 with the local field anisotropy data from [24] are also presented in figure 3. It is seen,

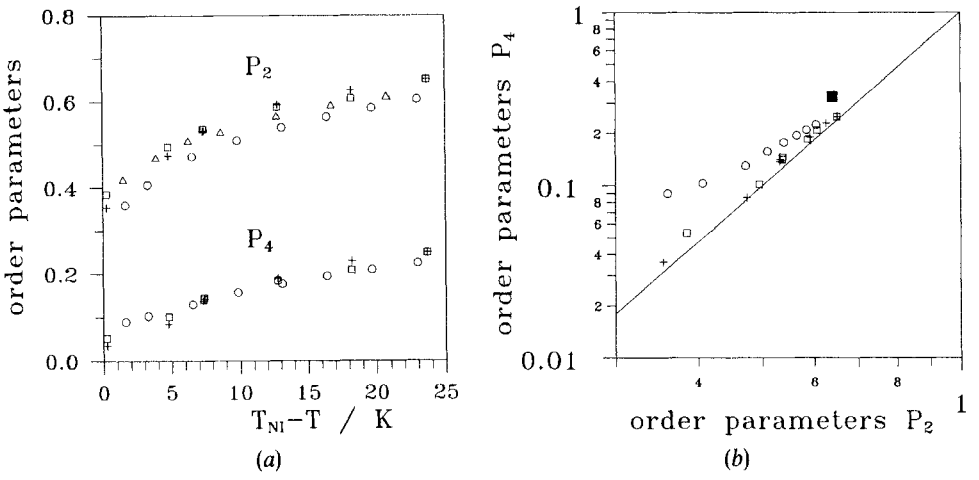

Figure 3. Temperature dependence of the order parameters of PCH5 obtained by IR dichroism measurements [20] (△), by Raman depolarization measurements—from Seeliger *et al.* [19], (○) and in this work ((□), in the isotropic local field approximation, +, accounting for the local field anisotropy) (*a*) and (*b*) and from computer simulations, (■). The straight line relates to the continuum theory predictions [24] (*b*).

that for PCH5 the local field anisotropy corrections are negligible over the range of existence of the mesophase. Although this agrees with other conclusions [4, 23], one should keep in mind that the local field can effect Raman band depolarization due not only to the macroscopic anisotropy of the mesophase, but also to thermal fluctuations [22] of the director in the mesophase. Although this effect can be noticeable for some substances [25], we will not discuss it here. But taking into account the coincidence of the $\langle P_2 \rangle$ order parameters obtained by Raman and absorption measurements (see figure 3 and the next section for explanations) for the same group, we shall adopt these values as the basis for the comparison with the simulation data.

From figure 3 one can conclude that as far as the order parameter $\langle P_2 \rangle$ is concerned, our simulation data reproduce well the experimental results in the temperature range $T_{NI} - T = 25$–30 K. There is the possibility [26] of scaling simulation data obtained for a microscopic volume to the limit of an infinite mesophase, but even for $\langle P_2 \rangle$, the lowest rank order parameter, this procedure is rather complicated, and for higher rank values the result of such scaling, if accessible, cannot be reliable. Therefore, we prefer simply to shift the temperature scale for the simulation data in the nematic phase and compare other statistical parameters with experimental results in the temperature range $T_{NI} - T = 25$–30 K.

Thus one can see that the simulated $\langle P_4 \rangle$ order parameters almost coincide with the experimental ones (within the errors of their determination, but somewhat higher than the experimental data). Of course, this discrepancy can be attributed to the improper scaling of the results: from figure 3 (*b*), it is evident that the simulation result on $\langle P_4 \rangle$ is a little higher than continuum theory predictions [27]. In this theory, the effect of the director fluctuations on the order parameters is explicitly taken into account. In our simulations, we suppress fluctuations with a half-period larger than the dimension of the box, i.e. with a wavevector smaller than approximately $10^7\,\mathrm{cm}^{-1}$. Allowing for such director fluctuations, one will obtain noticeable decrease of the order parameters, and $\langle P_4 \rangle$ should decrease faster than $\langle P_2 \rangle$ [28]. But, as is clear from

continuum theory, this changing of the order parameters will shift the point corresponding to the simulation results in figure 3 (*b*) parallel to the straight line, and it will not come closer to the experimental points.

It is evident from our previous considerations that there are also reasons for experimental $\langle P_4 \rangle$ data to be underestimated. Treatment of Raman data is based on the hypotheses of cylindrical symmetry of the molecules and the parallelism of the principal molecular and the polarizability derivative ellipsoid axes, and it is worth testing the validity of these assumptions. With the simulation data we have a unique possibility of computing the relative contributions of the terms of different symmetry.

The only symmetry property which can be accepted as a fact is the uniaxial macroscopic symmetry of the nematic phase. Because of molecular flexibility, there is no reason either to imply any symmetry of the molecules, or to refer to any intrinsic molecular frame. Hence we adopt as our molecule fixed frame the principal axes of the polarizability derivative tensor for the cyano vibration. Formulae for Raman intensities in this general case are cumbersome and therefore are presented in the Appendix. The number of non-trivial order parameters increases to 5, but that is less than $(2L+1)$ for each even rank L, due to the symmetry of the polarizability derivative tensor (for spontaneous Raman scattering, the anti-symmetric part is lacking). The polarizability derivative tensor in the frame we have chosen has 3 non-trivial components (see formulae (A 3)). The depolarization ratio measurements in the isotropic phase make it possible to relate two of them and to compute the intensities in units of the third (α_{00}, for example). Thus, calculated contributions of terms connected with various order parameters into Raman polarized intensities are depicted in figure 4.

It is obvious, that with the order parameters taken from the simulation data, it is impossible to fit the experimental results with any reasonable shape of polarizability derivative ellipsoid. Although small, the deviations are larger than experimental errors. And now the problem is not in the incompleteness of the set of order parameters: it is evident that many contributions related to molecular biaxiality could be neglected, but the main contributors (the isotropic term and those connected with $\langle P_2 \rangle$ and $\langle P_4 \rangle$) have relative values incompatible with experimental data. One possible reason is that due to the small dimensions of the simulation ensemble, fluctuations in it are suppressed and the higher rank order parameters have relatively high values. On the other hand, 'experimental' intensities depicted in figure 4 are computed on the basis of measurements for the isotropic phase. Due to molecular interactions, the polarizability derivative tensor can be deformed, and deformed to a different extent in different phases. This will lead to changes in the terms in (A 2) and to differences between the computed and experimental results. This seems to be the most probable reason, bearing in mind the somewhat different $\langle P_i \rangle$ obtained for different fragments within the rigid molecular core from Raman measurements [22].

We do not discuss here the non-coincidence effect of the principal axes of the polarizability derivative tensor with the molecular symmetry axes and the effects of molecular flexibility. We did not try to decouple and study them separately. But all of them implicitly contribute to the simulated order parameters. Some more words should be said about antiferroelectric packing of polar molecules [5]. Although its effect on the order parameters of simulated PCH5 is already included, but within the adopted interaction potential (only the cyano group possesses partial charges) it is negligible. Probably a more comprehensive treatment of the interaction potential may increase its contribution.

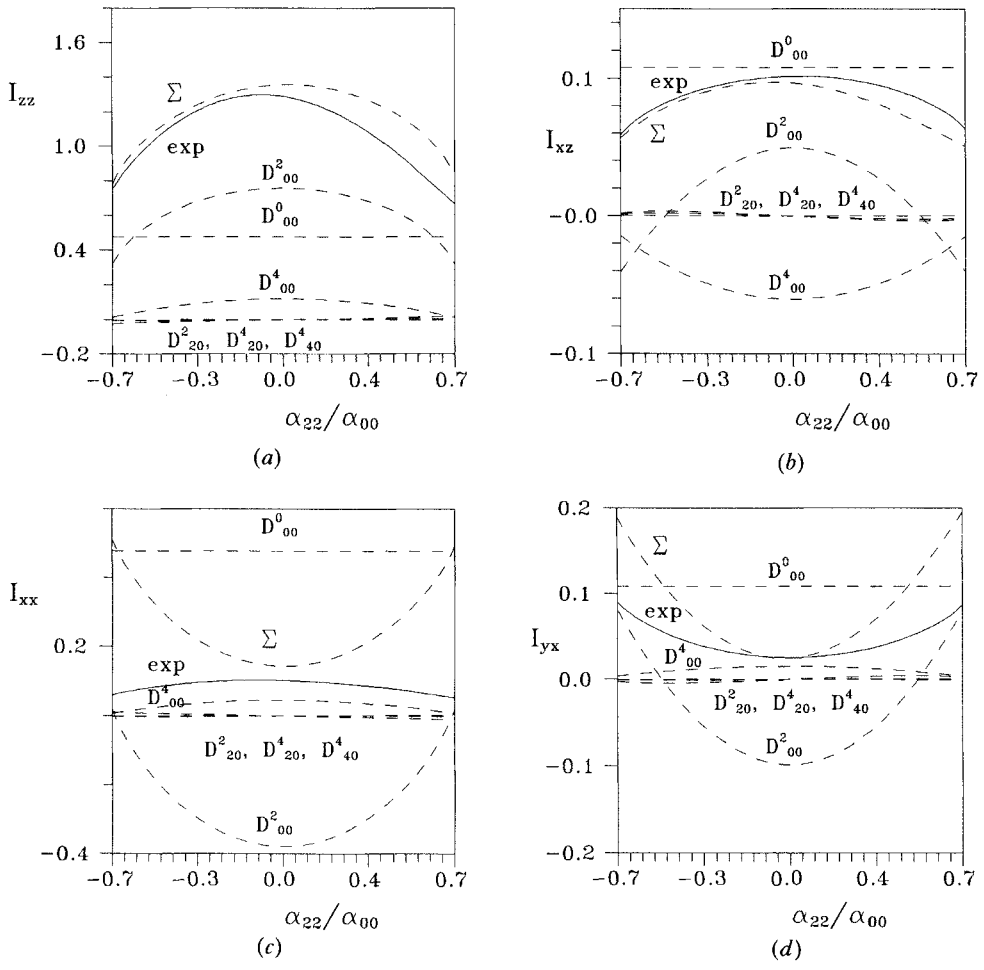

Figure 4. (*a*), (*b*), (*c*), (*d*) Contributions to the Raman intensity of the cyano stretching vibration in units of α_{22}/α_{00} from terms dependent on different order parameters (dashed lines). Σ is the total intensity of the polarized component which is compared to the experimental value (solid lines) calculated from Raman ratios and computed intensities (for example $I_{zz}=I_{xz}/R_1$). Experimental values of Raman ratios are taken from [22] at $T_{NI}-T=28$ K, and the order parameters from simulations (see the table).

3.2. *IR dichroism measurement*

Dichroism of the light absorption by liquid crystals is caused by the anisotropic distribution of transition moments, and when it is dipolar absorption, then its dichroism is determined by the second rank order parameters. For a uniaxial medium, consisting of asymmetric molecules, the dichroic ratio

$$N=\frac{k_z}{k_x}=\frac{n_x f_{zz}^2}{n_2 f_{xx}^2}\frac{1+2\langle D_{00}^2\rangle D_{00}^2+4\langle D_{02}^2\rangle D_{20}^2}{1-\langle D_{00}^2\rangle D_{00}^2-2\langle D_{02}^2\rangle D_{20}^2}, \tag{5}$$

depends only on two such parameters, $\langle D_{00}^2\rangle$ and $\langle D_{02}^2\rangle$ (the real parts of D-functions, as defined in the table), which can be determined by a proper choice of intramolecular vibrations [23]. Here, the Ds without angular brackets are related to the orientation of the dipole transition moment in the molecular reference frame. Usually, formula (5) is

written in terms of order parameters $\langle P_2 \rangle$ and D [23], which are connected to the Wigner functions through the relations

$$\langle P_2 \rangle = \langle D^2_{00} \rangle, \quad D = \sqrt{6} \langle D^2_{02} \rangle. \tag{6}$$

Dependence of the dichroism ratio on D appears in equation (5) only for asymmetric molecules due to different probabilities for their principal short axes to be aligned along the director. Other parameters in equation (5) such as refractive indices n_1 and local field factors f_{ii} arise from the macroscopic anisotropy of the medium and are usually determined by independent methods.

There are only a few publications dealing with the determination of both order parameters for liquid crystals, because of the difficulties of a proper choice of the vibrations under study. Kiefer *et al.* [23], determined such parameters for PCH7 and a mixture of PCH7 and PCH5. For both systems, the results are coincident within experimental error, and the $\langle P_2 \rangle$ for the last one are depicted in figure 3(*a*). The coincidence of this order parameter with Raman results assures us of the reliability of the data and makes it possible to compare D with simulation results in the same temperature interval as was used for $\langle P_4 \rangle$. Recalculating the D-parameter of [23], one can obtain from dichroism measurements $\langle D^2_{02} \rangle = 0{\cdot}012 \pm 0{\cdot}006$, which is almost coincident with the simulation result (see the table), keeping in mind experimental errors. Nevertheless, the tendency for simulated order parameters to be higher than experimental ones is observable.

Over estimation of the $\langle D^2_{02} \rangle$ order parameter in the simulation can have a similar origin to the over estimation of $\langle P_4 \rangle$. It has been observed, that simulated configurations tend to possess biaxiality. In such locally biaxial volumes, deflections of molecular long axes from the director orientation in the plane of the benzene ring are especially favourable. One can treat such microscopic volumes as spheres and their interactions are well described by the Maier–Saupe potential. Then, orientational disorder of microscopic volumes in the macroscopic volume of the liquid crystalline sample will strongly decrease the $\langle D^2_{02} \rangle$ order parameter, while having only a minor effect on $\langle P_2 \rangle$. Similar effects can be caused also by an antiferroelectric orientation of the molecules, which can be obtained with a more realistic model for the electrostatic interactions.

It should be noted, that there are several effects due to which experimental values of $\langle D^2_{02} \rangle$ can be distorted. We do not discuss here the local field macroscopic anisotropy effects. As shown in the previous section, for PCH5 they have almost no effect on the Raman data and the coincidence of $\langle P_2 \rangle$ from absorption measurements is encouraging. There is also some evidence from the treatment of absorption dichroism, that the local field anisotropy should not strongly affect $\langle D^2_{02} \rangle$ for PCH5. Such effects as molecular flexibility are also discounted, because we simulated flexible molecules and computed orientational statistics for those molecular fragments which were studied experimentally. But, as is evident from [23], dichroism data have a tendency to be different for different fragments even within the rigid core of the molecule. As checked by direct computations, this has no relevance to orientational statistics of these fragments. A systematically observed feature is that for vibrations of strongly polar cyano groups, the absorption dichroism is smaller than for a relatively weakly polarized benzene ring. This results in almost negligible changes in the $\langle P_2 \rangle$ derived from absorption data, but will lead to strong deviations during the derivation of $\langle D^2_{02} \rangle$. Such behaviour can be easily attributed to the effect of molecular interactions on the physical parameters of molecules [29] and should be treated explicitly.

4. Dynamic properties

Comprehensive information on the rotational movement of molecules in isotropic systems can be straightforwardly obtained from vibration–rotation Raman band-shape analysis [30]. Choosing appropriate Raman active vibrations and comparing Fourier transforms of the normalized spectral intensities for isotropic and anisotropic scattering

$$\left.\begin{aligned} C_{\mathrm{iso}}(t) &= C_{\mathrm{vib}}(t), \\ C_{\mathrm{anis}}(t) &= C_{\mathrm{vib}}(t)\sum a_{2\mathrm{m}}\alpha_{2\mathrm{n}}\langle D^2_{\mathrm{mn}}(t)\rangle \Big/ \sum a_{2\mathrm{m}}\alpha_{2\mathrm{n}}\langle D^2_{\mathrm{mn}}(0)\rangle, \end{aligned}\right\} \tag{7}$$

one can deduce different orientational auto-correlation functions $\langle D^2_{\mathrm{mn}}(t)\rangle$ which are in fact auto-correlators of Wigner D-functions connecting actual molecular orientation with that at $t=0$. Here

$$C(t) = \int dw I(w)\exp(-iwt) \Big/ \int dw I(w),$$

$$I_{\mathrm{iso}} = I_{\mathrm{vv}} - \tfrac{4}{3} I_{\mathrm{vh}}, \qquad I_{\mathrm{anis}} = I_{\mathrm{vh}},$$

where I_{vv} and I_{vh} are plane polarized Raman intensities with polarizations coincident and orthogonal, respectively with that of the exciting light. $C_{\mathrm{vib}}(t)$ is the time auto-correlation function of intramolecular vibration. As is evident from computer simulations and Raman depolarization studies, we can adopt axial symmetry for the polarizability derivative tensor of the cyano stretching vibration. Fixing the molecular frame with it, one can readily obtain $\langle D^2_{00}(t)\rangle$ for the isotropic phase (see figure 5). For mesogenic substances, the only difficulty is the very slow orientational relaxation of the molecules in comparison to their vibrational relaxation. Therefore some comments should be made on the peculiarities of the experimental method.

The experimental set-up for Raman studies and the preparation of liquid crystalline samples are thoroughly described elsewhere [31]. The only difference from the present study is the somewhat smaller slit width (HWHH is $2\,\mathrm{cm}^{-1}$) and higher laser power (150 mW) permissible for non-resonant Raman studies. The Raman spectrum was registered in the interval 1975–2475 cm^{-1} and within it only one additional band was observable with an intensity two orders of magnitude lower than that of the cyano stretch. For the background subtraction, we compared two methods. Firstly, intervals of $150\,\mathrm{cm}^{-1}$ on both edges of this range were fitted by a straight line. Secondly, we performed least-squares fitting of the whole interval by a lorentzian with a straight line background. The difference in the two resulting orientational correlation functions lies within the experimental error denoted by the vertical bars in figure 5.

Despite the relatively long time of spectrum accumulation, the experimental orientational auto-correlation function shows a large scattering of points. Nevertheless, its non-exponential behaviour on a short time-scale is readily observed. It disappears only if we use for the Fourier transform of the spectrum an interval smaller than $64\,\mathrm{cm}^{-1}$. The similar behaviour of the auto-correlation function obtained from simulation data convinces one that it is not an artifact. From experiment, it is impossible to decide, if such short-time behaviour is due to suppressed librational molecular motion or if on different time scales one observes different relaxation mechanisms (single-molecule orientational relaxation in the relatively stable cage formed by its neighbours at short times and relaxation of this cage at long times, for example).

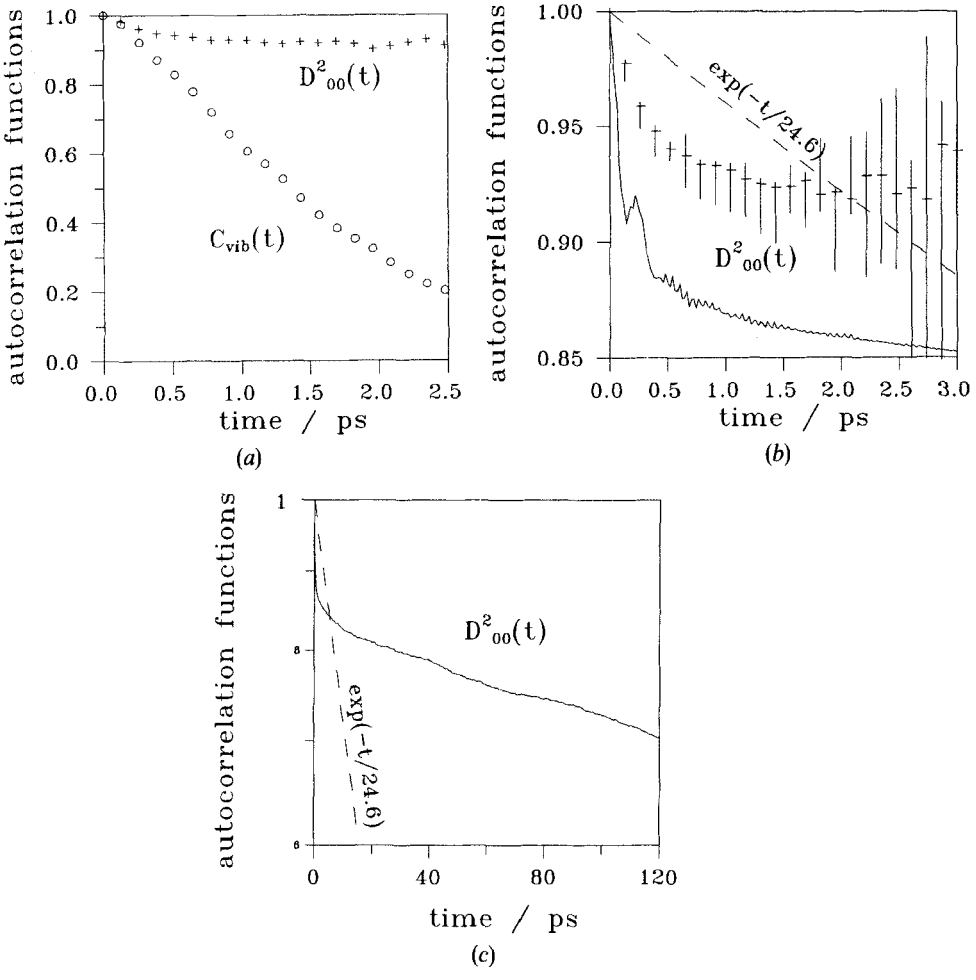

Figure 5. (*a*), (*b*), (*c*) Vibrational and orientational auto-correlation functions for PCH5 for the isotropic phase obtained from experiment (symbols) and from computer simulations (solid lines). Dashed line is the result obtained from Raman band-width measurements in the small-step diffusion approximation.

Although the divergence of experimental and simulated correlation functions is obvious, we should mention that correlation functions obtained with realistic interaction potentials decay much more slowly than those of ellipsoidal models [1]. The origin of the residual discrepancy is not totally clear. Attributing the fast initial decay to librational motion suggests a slightly larger average libration angle in the simulation, compared to the real liquid (about 15° versus about 10°). For the derivation of relations (7), only few assumptions have been made: the absence of correlations between vibrations and rotations and between vibrations of different molecules. For such a high-frequency characteristic vibration as the cyano stretch in such large molecules, this assumption is a priori valid. It has been also supposed that there is no collision induced scattering. Keeping in mind the relatively small difference between the isotropic and anisotropic components, which should be detected for studies of the orientational movement of mesogenic molecules, this assumption is difficult to check.

What is clear is the fact that we cannot attribute this phenomenon to the effect of conformational flexibility of the mesogen molecule, because in both cases the rotation of the same fragment was under study.

For anisotropic systems, the situation is substantially complicated by the lowering of orientational symmetry: the number of independent orientational correlation functions $\langle D^2_{mn}(t)D^2_{pq}(0)\rangle$ increases (here the Wigner D-functions connect molecular and laboratory reference frames). Even for the simplest case of a uniaxial mesophase, constituted of cylindrically symmetric molecules ($m=p$, $n=q$), there are 9 non-vanishing functions with different non-negative m and n [32], while the number of independent polarized Raman components is only four [33]

$$\left.\begin{aligned}
C_{zz}(t) &= |\alpha_{00}|^2 + 2\sqrt{\left(\frac{2}{3}\right)}\alpha_{00}\alpha_{20}\langle P_2\rangle + \frac{2}{3}\sum_{m=-2}^{2}|\alpha_{2m}|^2\langle D^2_{0m}(t)D^2_{0m}(0)\rangle,\\
C_{xx}(t) &= |\alpha_{00}|^2 - \sqrt{\left(\frac{2}{3}\right)}\alpha_{00}\alpha_{20}\langle P_2\rangle + \frac{1}{6}\sum_{m=-2}^{2}|\alpha_{20}|^2\langle D^2_{0m}(t)D^2_{0m}(0)\rangle\\
&\quad + \frac{1}{2}\sum_{m=-2}^{2}|\alpha_{2m}|^2\langle D^2_{2m}(t)D^2_{2m}(0)\rangle,\\
C_{xz}(t) &= \frac{1}{2}\sum_{m=-2}^{2}|a_{2m}|^2\langle D^2_{1m}(t)D^2_{1m}(0)\rangle,\\
C_{xy}(t) &= \frac{1}{2}\sum_{m=-2}^{2}|\alpha_{2m}|^2\langle D^2_{2m}(t)D^2_{2m}(0)\rangle,
\end{aligned}\right\} \quad (8)$$

where the z axis is coincident with the symmetry axis of the mesophase. Therefore, to extract useful information, one has to proceed with additional approximations.

Although during the treatment of the isotropic phase system the non-exponential decay of the auto-correlation function has been demonstrated, we shall start the analysis of the rotational movement in the nematic phase with an approach developed in reference [33] on the basis of the small step rotational diffusion model. In this case, reorientational motion is described by single exponenital time correlation functions $\langle D^2_{mn}(t)D^2_{pq}(0)\rangle$ [34]. By modifying the diffusion equations to account for the presence of an orienting potential and assuming that this potential is of mean field type, one can derive explicit expressions for $\langle D^2_{mn}(t)D^2_{mn}(0)\rangle$ in terms of rotational diffusion constants (keeping in mind the discussion of static parameters, we shall neglect molecular biaxiality). For determination of the relaxation times of these auto-correlation functions, it is even unnecessary to perform Fourier transforms of the Raman band contour. All useful information can be obtained from band width measurements [8] for suitably selected modes. For example, the band-widths of the polarized Raman components for the cyano stretching vibration, in the approximation of a cylindrically symmetric polarizability ellipsoid (in the molecule fixed frame), are dependent only on one orientational diffusion constant D_r connected with molecule tumbling [8]

$$\left.\begin{aligned}
\delta_{xz} &= \delta_{vib} + \frac{6}{\pi c}D_r(7 + \tfrac{5}{2}\langle P_2\rangle + 8\langle P_4\rangle)/(7 + 5\langle P_2\rangle - 12\langle P_4\rangle),\\
\delta_{zz} &= \delta_{vib} + \frac{8}{3\pi c}D_r(7 + 5\langle P_2\rangle - 12\langle P_4\rangle)/(7 + 20\langle P_2\rangle + 8\langle P_4\rangle),\\
\delta_{xx} &= \delta_{vib} + \frac{8}{3\pi c}D_r(7 - \tfrac{5}{2}\langle P_2\rangle - \tfrac{9}{2}\langle P_4\rangle)/(7 - 10\langle P_2\rangle + 3\langle P_4\rangle).
\end{aligned}\right\} \quad (9)$$

Here δ_{vib} is the contribution of the vibrational relaxation to the total band-width. Fitting the cyano Raman vibration band by a Lorentzian for band-width determination (see figure 6), we have calculated with relations (9) D_r and the orientational correlation times for some correlation functions which contribute to the band-shape under study in the approximations adopted here

$$\left.\begin{aligned}\tau_{00}&=\frac{7+10\langle P_2\rangle+18\langle P_4\rangle-35\langle P_2\rangle^2}{(7+5\langle P_2\rangle-12\langle P_4\rangle)6D_r},\\ \tau_{10}&=\frac{7+5\langle P_2\rangle-12\langle P_4\rangle}{(7+2{\cdot}5\langle P_2\rangle+8\langle P_4\rangle)6D_r},\\ \tau_{20}&=\frac{7-10\langle P_2\rangle+3\langle P_4\rangle}{(7-5\langle P_2\rangle-2\langle P_4\rangle)6D_r}.\end{aligned}\right\} \tag{10}$$

Comparing figures 7 and 8 one can conclude that, while the relative values of τ_{10} and τ_{20} are in reasonable agreement with simulation data, the absolute values for all experimental correlation times are substantially lower than those for the simulated system. And it is evident from figure 8, that the main reason for this is the non-exponential or multi-exponential behaviour of the orientational auto-correlation functions at short time-scale. This non-exponentiality originates, not from the macroscopic anisotropy (it is also observable for the isotropic phase in figure 5), but probably from hindered motions in the relaxing cage constituted by surrounding molecules. Nevertheless, to clarify this and to make numerical estimates, one should probably study the dynamics of many-particle correlation functions.

One remarkable feature which can be observed from band-width analysis is the negligibility of the rotational contribution to the broadening of zz component of the cyano Raman vibration band. As is seen from figure 6 (*b*), it is approximately ten times smaller, than that of the xz component. This, of course, does not mean that the relaxation time for $\langle D^2_{00}(t)D^2_{00}(0)\rangle$, which contributes to the zz component, should be as

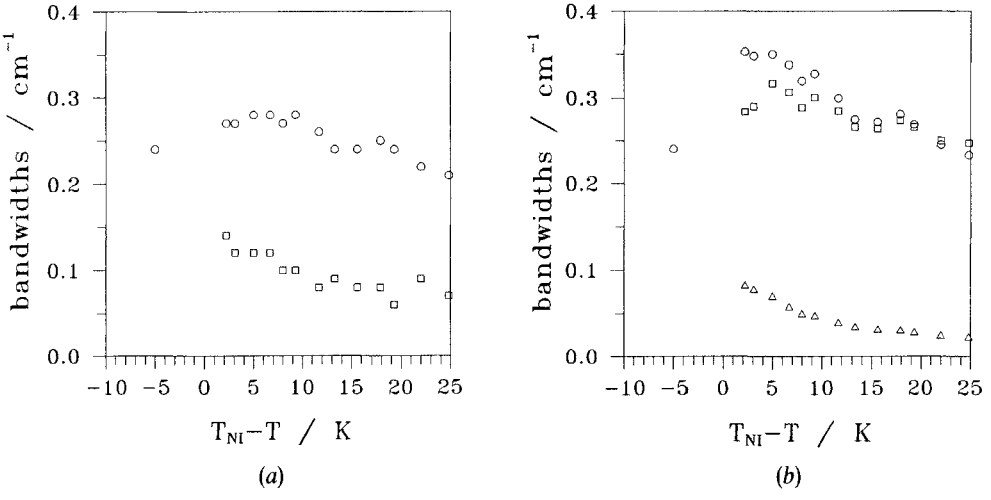

Figure 6. Temperature dependence of the differences of (*a*) the bandwidths of the polarized components: (□), $\delta_{zx}-\delta_{xx}$, (○), $\delta_{zx}-\delta_{zz}$; and of (*b*) the rotational contributions to the bandwidths (HWHH) calculated with equation (9), using experimental data for $\delta_{zx}-\delta_{zz}$ to determine D_r: (○), δ_{zx}, (△), δ_{zz}, (□), δ_{xx}.

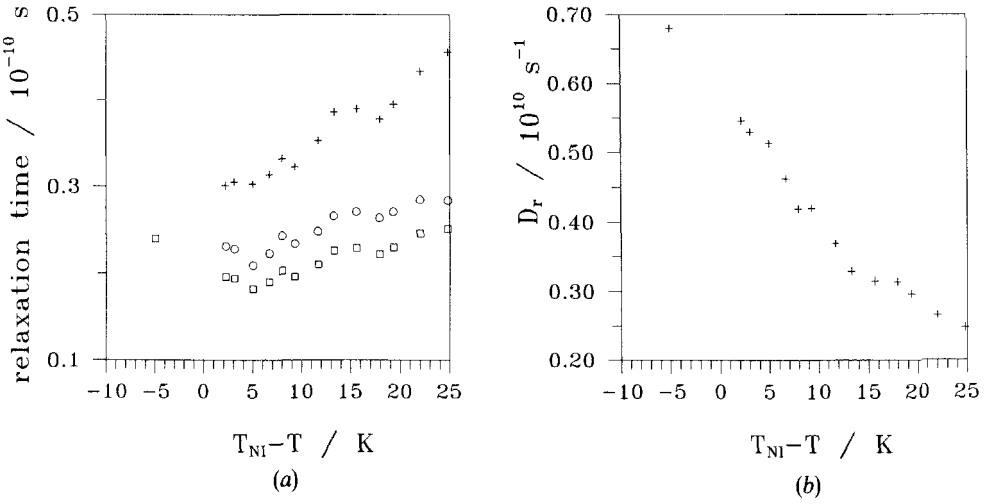

Figure 7. Temperature dependence of orientation auto-correlation times (*a*) (○) τ_{00} (+) τ_{10} (□) τ_{20} and orientational diffusion coefficient (*b*) in the nematic phase of PCH5 determined from Raman bandwidth measurements.

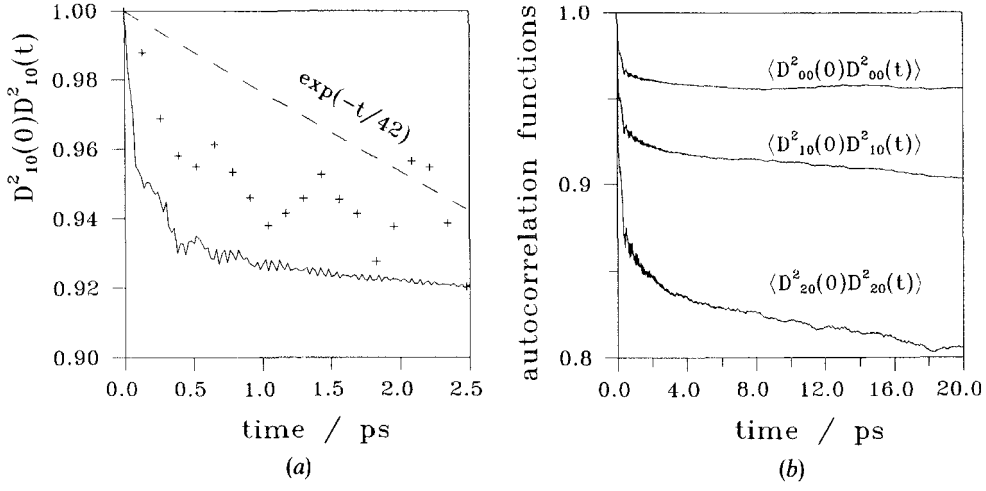

Figure 8. (*a*), (*b*) Orientational auto-correlation functions for PCH5 in the nematic phase at $T_{NI} - T = 25$ K, obtained from Raman band-shape analysis (symbols) and from simulations (solid lines).

much larger than that for $\langle D^2_{10}(t)D^2_{10}(0)\rangle$, which contributes to the xz component of the cyano Raman band. As is clear from simulation data (see figure 8 (*b*)), these correlation functions are not so greatly different. One can see from equations (8), that this is due principally to the different dependence of these polarized components on the rotational motion. Hence, analysing molecular reorientation in the nematic phase, we can reject the diffusion model and use equations (8) in truncated form. Therefore we adopt cylindrical symmetry for both the PCH5 molecule and the polarizability derivative ellipsoid (in equations (8) this means that $m=0$) and neglect the last term in $C_{zz}(t)$. The so derived $\langle D^2_{10}(t)D^2_{10}(0)\rangle$ is compared in figure 8 (*a*) to the simulated result.

Despite the strong scattering of experimental points due to the small contribution of rotational motion to the broadening of mesogen Raman bands and due to relatively fast vibrational relaxation, the non-exponential behaviour of the orientational correlation function is observed also in the mesophase. The main conclusion which can be drawn from the comparison of the time correlation functions obtained from Raman measurements with simulated ones is the fact that the use of diffusion models for the treatment of the Raman data leads to a substantial over estimation of the orientational diffusion coefficient for tumbling motion. How large this difference can be is evident from comparison of the long-time behaviour of the simulated correlation function compared with that obtained from Raman band-width measurements for the isotropic phase, where the non-exponentiality is the only reason for these curves being different (see figure 5 (*c*)). Raman band-width measurements are sensitive only to the short-time (4–5 ps) behaviour of the correlation function and therefore, in our case, they give an approximately 20 times larger slope of the exponent (and consequently of the orientational diffusion coefficient) than that observed at longer times for the simulated correlation function. This helps to explain the large difference in orientational relaxation times obtained experimentally from Raman and luminescence measurements [35]. The closer agreement of the orientational auto-correlation functions in the nematic phase compared to the isotropic phase suggests that neglecting orientational disorder, the small dimensions of the box used in the simulations are already felt in the dynamic behaviour.

5. Conclusions

Summarizing the results on both static and dynamic properties in the isotropic and nematic phases, it is possible to conclude, that using site–site interaction potentials one can achieve rather good agreement between real and simulated systems. To improve the agreement of these parameters simultaneously, dynamic properties of the simulated system must be shifted towards the lower temperature region, while the static properties should be those more characteristic for high temperature systems. This can be done only by introducing new terms in the interaction potential. First of all, electrostatic interactions should be accounted for more comprehensively. They, and also induction interactions [36], will lead to the formation of more pronounced antiferroelectric packing of molecules and consequently to decrease in the order parameters. On the other hand, these long-range interactions will slow down molecular movement, especially its short-time behaviour, which in our system looks like free rotation through larger angles. The explicit treatment of H-atom repulsions, which result in 'roughening' of the molecules, will have the same effect. Such changes, of course, will necessitate changes in the interaction parameters adopted in our model and which have essentially a phenomenological nature. As a more precise description of the thermodynamic or phase transition parameters is desirable, one should start with an increase in size of the simulation box. But even without doing this and only scaling the simulated data, it is possible to clarify many spectroscopic experimental situations. For the system under study, we can conclude that while the isotropy of the local field is evident, the direct effect of molecular interactions on the optical parameters is noticeable.

Financial support from Deutsche Forschungsgemeinschaft and E. Merck, Darmstadt is gratefully acknowledged. We also thank Professor Dr J. Pelzl (Bochum) for making possible the performance of the Raman measurements for this work and we thank HLRZ Juelich for a generous amount of computer time.

Appendix

Three independent Raman ratios

$$r_1=\frac{\langle\gamma_{xz}^2\rangle}{\langle\gamma_{zz}^2\rangle},\quad r_2=\frac{\langle\gamma_{zx}^2\rangle}{\langle\gamma_{xx}^2\rangle},\quad r_3=\frac{\langle\gamma_{yx}^2\rangle}{\langle\gamma_{xx}^2\rangle}, \tag{A 1}$$

for a uniaxial medium (with axis along z) are determined by the average over all orientations of the square of the components of the polarizability derivative tensor

$$\left.\begin{aligned}
\langle\gamma_{zz}^2\rangle&=[\tfrac{1}{3}\alpha_{00}^2+\tfrac{2}{15}\alpha_{20}^2+\tfrac{4}{15}\alpha_{22}^2]+[\tfrac{2\sqrt{2}}{3}\alpha_{00}\alpha_{20}+\tfrac{4}{21}\alpha_{20}^2+\tfrac{8}{21}\alpha_{22}^2]\langle D_{00}^2\rangle\\
&\quad+[\tfrac{4\sqrt{2}}{3}\alpha_{00}\alpha_{22}-\tfrac{16}{21}\alpha_{20}\alpha_{22}]\langle D_{02}^2\rangle+[\tfrac{12}{35}\alpha_{20}^2+\tfrac{2}{105}\alpha_{22}^2]\langle D_{00}^4\rangle\\
&\quad+\tfrac{8\sqrt{3}}{7\sqrt{5}}\alpha_{20}\alpha_{22}\langle D_{02}^4\rangle+\tfrac{4\sqrt{2}}{\sqrt{35}}\alpha_{22}^2\langle D_{04}^4\rangle,\\
\langle\gamma_{xx}^2\rangle&=[\tfrac{1}{3}\alpha_{00}^2+\tfrac{2}{15}\alpha_{20}^2+\tfrac{4}{15}\alpha_{22}^2]+[-\tfrac{\sqrt{2}}{3}\alpha_{00}\alpha_{20}-\tfrac{2}{21}\alpha_{20}^2+\tfrac{8}{21}\alpha_{22}^2]\langle D_{00}^2\rangle\\
&\quad+[-\tfrac{2\sqrt{2}}{3}\alpha_{00}\alpha_{22}+\tfrac{8}{21}\alpha_{20}\alpha_{22}]\langle D_{02}^2\rangle+[\tfrac{9}{70}\alpha_{20}^2+\tfrac{2}{105}\alpha_{22}^2]\langle D_{00}^4\rangle,\\
&\quad+\tfrac{3\sqrt{3}}{7\sqrt{5}}\alpha_{20}\alpha_{22}\langle D_{02}^4\rangle+\tfrac{3\sqrt{2}}{2\sqrt{35}}\alpha_{22}^2\langle D_{04}^4\rangle,\\
\langle\gamma_{xz}^2\rangle&=[\tfrac{1}{10}\alpha_{20}^2+\tfrac{1}{5}\alpha_{22}^2]+[\tfrac{1}{14}\alpha_{20}^2-\tfrac{1}{7}\alpha_{22}^2]\langle D_{00}^2\rangle-\tfrac{2}{7}\alpha_{20}\alpha_{22}\langle D_{02}^2\rangle\\
&\quad-[\tfrac{6}{35}\alpha_{20}^2+\tfrac{2}{35}\alpha_{22}^2]\langle D_{00}^4\rangle-\tfrac{4\sqrt{3}}{7\sqrt{5}}\alpha_{20}\alpha_{22}\langle D_{02}^4\rangle-2\tfrac{\sqrt{2}}{\sqrt{35}}\alpha_{22}^2\langle D_{04}^4\rangle,\\
\langle\gamma_{yx}^2\rangle&=[\tfrac{1}{10}\alpha_{20}^2+\tfrac{1}{5}\alpha_{22}^2]-[\tfrac{1}{7}\alpha_{02}^2-\tfrac{2}{7}\alpha_{22}^2]\langle D_{00}^2\rangle+\tfrac{4}{7}\alpha_{20}\alpha_{22}\langle D_{02}^2\rangle\\
&\quad-[\tfrac{3}{70}\alpha_{20}^2+\tfrac{1}{70}\alpha_{22}^2]\langle D_{00}^4\rangle+\tfrac{1\sqrt{3}}{7\sqrt{5}}\alpha_{20}\alpha_{22}\langle D_{02}^4\rangle+\tfrac{\sqrt{2}}{2\sqrt{35}}\alpha_{22}^2\langle D_{04}^4\rangle,
\end{aligned}\right\} \tag{A 2}$$

where the order parameters (see the table) and circular components of the polarizability derivative tensor in the molecular reference frame are defined according to [18]

$$\left.\begin{aligned}
\alpha_{00}&=-\tfrac{1}{\sqrt{3}}(\alpha_{xx}+\alpha_{yy}+\alpha_{zz}),\\
\alpha_{20}&=-\tfrac{1}{\sqrt{6}}(2\alpha_{zz}-\alpha_{yy}-\alpha_{xx}),\\
\alpha_{22}&=\tfrac{1}{2}(\alpha_{yy}-\alpha_{xx}),
\end{aligned}\right\} \tag{A 3}$$

and the symmetry and diagonality of the polarizability derivative tensor in the molecular reference frame are taken into consideration. For the isotropic phase, the Raman depolarization ratio is readily derived from any one of the ratios (A 1) by equating all the order parameters to zero.

References

[1] Zannoni, C., and Guerra, M., 1981, *Molec. Phys.*, **4,** 849.
[2] Emerson, A. P. J., Hashim, R., and Luckhurst, G. R., 1992, *Molec. Phys.*, **76,** 241.
[3] Jen, S., Clark, N. A., Pershan, P. S., and Priestly, E. B., 1977, *J. chem. Phys.*, **66,** 4635.
[4] Dalmolen, L. G. P., and de Jeu, W. H., 1983, *J. chem. Phys.*, **78,** 7353.
[5] Picken, S. J., van Gunsteren, W. F., van Duijnen, P. Th., and de Jeu, W. H., 1989, *Liq. Crystals*, **6,** 357.
[6] Sinton, S. W., Sax, D. B., Murdoch, J. B., and Pines, A., 1984, *Molec. Phys.*, **53,** 333.
[7] Beckmann, P. A., Emsley, J. W., Luckhurst, G. R., and Turner, D. L., 1983, *Molec. Phys.*, **50,** 699.
[8] Kirov, N., Dozov, I., Rosi, B., and Fontana, M. F., 1988, *J. molec. Struct.*, **173,** 173.
[9] Dozov, I., Kirov, N., and Petroff, B., 1987, *Phys. Rev.* A, **36,** 2870.
[10] Lalanne, J. R., Martin, B., Pouligny, B., and Kielich, S., 1977, *Molec. Crystals liq. Crystals*, **42,** 153.
[11] Reid, C. J., and Evans, M. W., 1980, *Molec. Phys.*, **40,** 1357.
[12] Humphries, R. L., James, P. G., and Luckhurst, G. R., 1972, *J. chem. Soc. Faraday Trans. II*, **68,** 1031.

[13] FRANKLIN, W., 1977, *Molec. Crystals liq. Crystals*, **40,** 91.
[14] WILSON, M. R., and ALLEN, M. P., 1991, *Molec. Crystals liq. Crystals*, **198,** 465.
[15] ONO, I., and KONDO, S., 1991, *Molec. Crystals liq. Crystals Lett.*, **8,** 69.
[16] WILSON, M. R., and ALLEN, M. P., 1992, *Liq. Crystals*, **12,** 157.
[17] ZANNONI, C., 1979, *The Molecular Physics of Liquid Crystals*, edited by G. R. Luckhurst and G. W. Gray (Academic Press), Chap. 3.
[18] VARSHALOVICH, D. A., MOSKALEV, A. N., and KHERSONSKII, V. K., 1988, *Quantum Theory of Angular Momentum* (*World Scientific*), Chap. 1–4.
[19] GROMOS, *Groningen Molecular Simulation* is a software package developed by W. F. van Gunsteren and H. J. C. Berendsen, University of Groningen, 1987.
[20] KRÖMER, G., PASCHEK, D., and GEIGER, A., 1993, *Ber. Bunsenges. phys. Chem.*, **97,** 1188.
[21] RYKAERT, J. P., CICOTTI, G., and BERENDSEN, H. J. C., 1977, *J. comput. Phys.*, **23,** 327.
[22] SEELIGER, R., HASPECLO, H., and NOACK, F., 1983, *Molec. Phys.*, **49,** 1039.
[23] KIEFER, R., and BAUR, G., 1989, *Molec. Crystals liq. Crystals*, **174,** 101.
[24] YAKOVENKO, S. YE., IGNATOVICH, R. R., PELZL, J., and MÜLLER, S., 1992, *Liq. Crystals*, **12,** 973.
[25] YAKOVENKO, S. YE., 1987, *Zh. Prikl. Spektrosk.*, **47,** 779.
[26] FABER, T. E., 1991, *Liq. Crystals*, **9,** 95.
[27] FABER, T. E., 1977, *Proc. R. Soc.* A, **353,** 247.
[28] SHENG, P., 1976, *Solid St. Commun.*, **18,** 1165.
[29] MINKO, A. A., NAUMENKO, V. I., and YAKOVENKO, S. YE., 1986, *Zh. Prikl. Spektrosk.*, **44,** 82; 1986, *Ibid.*, **44,** 271.
[30] MCCLUNG, R. E. D., 1977, *Advances in Molecular Relaxation and Interaction Processes*, Vol. 10 (Elsevier), p. 83.
[31] YAKOVENKO, S. YE., IGNATOVICH, R. R., MULLER, S., and PELZL, J., 1991, *Liq. Crystals*, **10,** 821.
[32] ZANNONI, C., 1979, *Molec. Phys.*, **38,** 1813.
[33] KIROV, N., DOZOV, I., and FONTANA, M. P., 1985, *J. chem. Phys.*, **83,** 5267.
[34] NORDIO, P. L., and SEGRE, U., 1979, *The Molecular Physics of Liquid Crystals*, edited by G. R. Luckhurst and G. W. Gray (Academic Press), p. 411.
[35] RATCHKEVITCH, W. S., YAKOVENKO, S. YE., and PELZL, J., 1992, *Proceedings of the Thirteenth International Conference on Raman Spectroscopy, Würzburg* (John Wiley & Sons) p. 422.
[36] BUCKINGHAM, A. D., 1967, *Adv. chem. Phys.*, **12,** 167.